

## **Design, fabrication and performance characterization of a miniature PEMFC stack based on MEMS technology**

*Xigui Zhang<sup>1,2,\*</sup>, Tao Wang<sup>1,2</sup>, Dan Zheng<sup>1,3</sup>, Jian Zhang<sup>1</sup>, Yao Zhang<sup>1</sup>, Ling Zhu<sup>1</sup>, Cong Chen<sup>1</sup>, Jian Yan<sup>1</sup>, Haohan Liu<sup>1</sup>, Yuwan Lou<sup>1</sup>, Xinxin Li<sup>1</sup>, Baojia Xia<sup>1</sup>*

<sup>1</sup>Shanghai Institute of Microsystem and Information Technology, Chinese Academy of Sciences, Shanghai 200050, China

<sup>2</sup>Shanghai Institute of Shanghai 200381, China

<sup>3</sup>Shanghai Institute of Technology, Shanghai 200233, China

\*E-mail: [zhangxigui@mail.sim.ac.cn](mailto:zhangxigui@mail.sim.ac.cn)

*Received: 10 June 2007 / Accepted: 9 July 2007 / Published: 1 August 2007*

In this study, the design, fabrication and performance characterization of a miniature 6-cell PEMFC stack based on MEMS technology was carried out. A novel type of Z-type anode flow field plates were applied to replace the full pin-type ones used previously and all the single cells were assembled in the same plane with a fuel buffer/distributor as their support. Operating on dry H<sub>2</sub> and air-breathing conditions at 20±3°C and 50±3% RH, the stack produced the peak power of 1.34W and the estimated maximum power density of the stack could reach 335W/L when the stack's volume of 4.0ml was considered. Meanwhile, all the single cells in the stack performed well and even based on V-I and internal resistance measurement (EIS). The results suggested that the stack's performance was greatly improved compared with the previous work. The novel Z-type anode flow field leading to more even fuel distribution among each cell probably had the greatest contribution for the improvement.

**Keywords:** PEMFC stack design; MEMS technology; Fuel buffer/distributor; Z-type anode flow field; Air-breathing

### **1. INTRODUCTION**

In recent years, many researchers have put their effort into fabrication of micro/miniature fuel cells ( $\mu$ FCs) or its components [1-15]. This is because  $\mu$ FCs are widely considered to be a major candidate for the micro scale power generation with higher energy densities than the most competitive rechargeable batteries, Li-ion and Ni-MH batteries in particular. However, apart from the good designs and advanced materials, miniaturizing fuel cells for micro scale power source is actually hindered by difficulty of reducing its physical dimensions because macro-sized fuel cell components (such as bipolar plates and fuel storage cans) are often limited by their characteristic fabrication technology

constraints, especially when it comes to the one or less Watt of  $\mu$ FCs. Thanks to Micro-Electronic-Mechanical-System (MEMS) technology, micro-channel patterns of  $\mu$ FCs bipolar plates into which reactants are fed and other components (such as micro fuel reformers/processors [7,12,13] and micro pumps[3]) can be fabricated on a silicon wafer with high resolution and good reproducibility. It has been demonstrated that MEMS technology is one of the most promising technologies for fuel cell miniaturization and integration. However, a lot of work was focused only on using such technology for fabrication of the single cell [2, 8, 9]. In fact, for the practical uses, several or even hundreds of single cells needed to be serially grouped or integrated to offer the required voltage and power. From our knowledge, there were only a few of stacks fabricated by MEMS technology were reported or proposed [14-16]. For example, Lee et al. [14] reported a micro fuel cell stack in which a planar array of cells is serially connected in a “flip-flop” configuration. The peak power in a 4-cell silicon assembly was reported to reach  $40 \text{ mW/cm}^2$  using hydrogen and oxygen as fuel and oxidizer. Yu et al. [15] fabricated a miniature twin fuel cells connected in series by sandwiching two membrane-electrode assemblies between two silicon micro-machined plates. The electricity interconnection from the cathode of one cell to the anode of another cell is made in the same plane and the interconnection was fabricated by sputtering a layer of copper over a layer of gold on the top of the silicon wafer. The measured peak power density was  $190.4 \text{ mW/cm}^2$  at  $270 \text{ mA/cm}^2$  when operating on dry  $\text{H}_2 / \text{O}_2$  at  $25^\circ\text{C}$  and atmospheric pressure.

In this study, Design, fabrication and performance characterization of a MEMS-based 6-cell PEMFC stack was investigated. A novel anode flow field plates for the stack and a fuel buffer/distributor were fabricated by a classical MEMS etching and silicon-glass bonding technologies respectively. Each cell was made by sandwiching a membrane-electrode-assembly (MEA) between two flow field plates and they were assembled in the same plane with a fuel buffer/distributor as their support. Performance and electrochemical resistance characterization of the stack were done by the linear polarization and Electrochemical Impedance spectroscopy (EIS) under dry hydrogen and air-breathing conditions for the cathode.

## 2. EXPERIMENTAL PART

### 2.1. Design of the stack

The MEMS-based 6-cell stack was made by assembling the 6 cells in the same plane with a fuel buffer/distributor as their support. The fuel buffer/distributor was fabricated by a silicon-glass bonding technology. Each cell was fabricated by sandwiching the home-made MEA between two silicon wafer-based flow field plates with active area of  $1.44 \text{ cm}^2$ . Two strips of the cells were arranged with 3 cells in a row. Fuel from the hydrogen source is first flowing into chamber of the fuel buffer/distributor, then distributing to each cell through the holes formed in the Pyrex glass. A C-type channel collects exhaust gases from the 6 cells and drain them out from the outlet hole formed on the silicon wafer. The structure diagram of the 6-Cell MEMS-based PEMFC stack is schematically shown in Fig. 1.

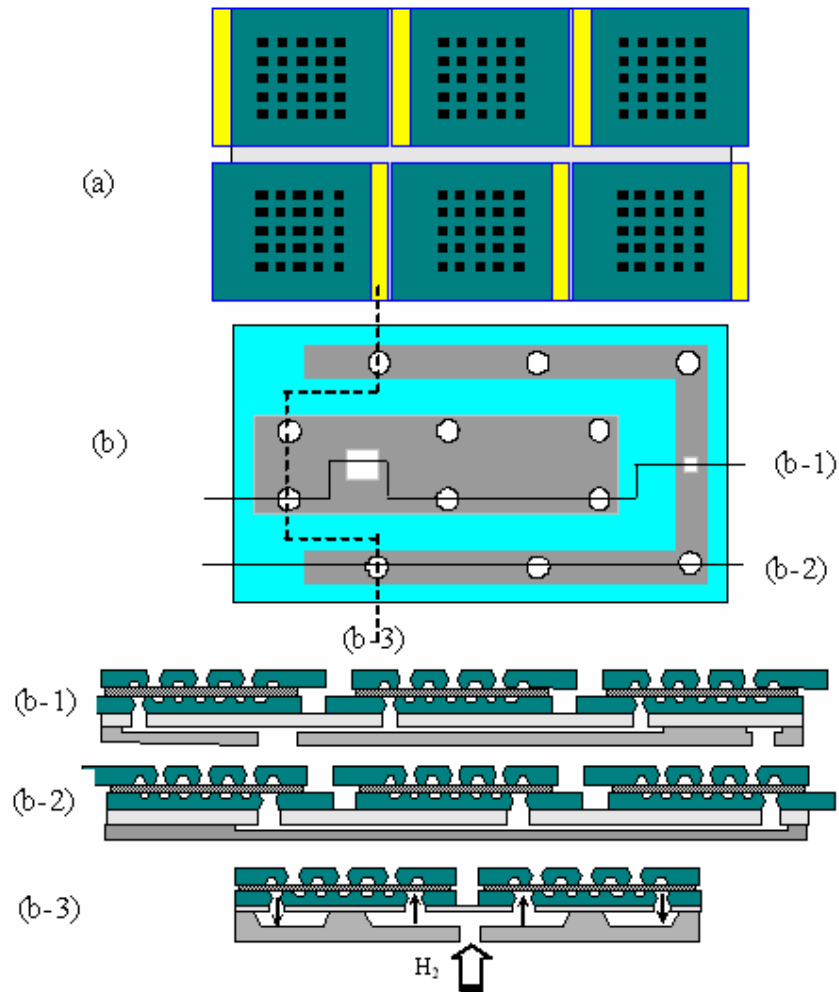


**Figure 1.** The schematic structure diagram of the 6-Cell MEMS-based PEMFC stack

## 2.2. Fabrication of the flow field plates of Z-type anode and air-breathing cathode

A 4 inch,  $525\pm20\mu\text{m}$ -thick N-type  $<1\ 0\ 0>$  silicon wafer with resistance ratio ranging from 1.5 to  $2.5\Omega\cdot\text{cm}$  was used as the original material in this work. The fabricating processes was briefly introduced as follow: (1) Heat deposit of a silicon dioxide layer on the wafer used as a silicon etch mask; (2) Photolithography of the mask windows on the back of the wafer; (3) Heat deposit of a silicon dioxide layer again to form the different thick layers on the back of the wafer; (4) Photolithography of the mask windows on the front of the wafer; (5) Etch of the front wafer in 40wt% KOH solution at  $50^\circ\text{C}$  and the etching depth was controlled at  $100\mu\text{m}\pm2\mu\text{m}$ ; (6) Wash the wafer in BOE solution (4 portions of 40%  $\text{NH}_4\text{F}$  and 6 of 49% HF mixture solution); (7) Double sides wet etch the wafer in KOH solution again to form the pin-type flow field patterns with two square through holes for the hydrogen plates and the through holes flow field patterns for the oxygen plates; (8)

Remove the residual silicon dioxide on the surface of the wafer; (9) Heat deposit of continuous silicon dioxide layers for electrical insulation; (10) Sputtering a Ti/Pt/Au composite metal layers on the wafer surface to act as conductive layer and ensure the metal layers would bond well in contact with the silicon wafer. The thickness of Ti, Pt and Au layer was controlled at  $0.1\mu\text{m}$ .  $0.3\mu\text{m}$  and  $0.5\mu\text{m}$  respectively. The flow field patterns of the anode are a array of pin-type isolated ‘isles’ and two through pseudo-square holes for fuel in and out. The isle is about  $293\times293\mu\text{m}^2$  on top and  $300\mu\text{m}$  in depth. Note that two pieces of micro grooves measuring  $8\text{cm}$  were formed simultaneously (Fig. 2a).The through hole for hydrogen in is about  $1.5\times1.5\text{mm}^2$  and that for hydrogen out is about  $0.5\times0.5\text{mm}^2$  respectively. The flow field pattern of the cathode is an array of pin-type isolated through ‘isles’ using for air-breathing (Fig. 2b). The dimension of the flow field plate is about  $1.6\times1.8\text{cm}^2$  with active area of  $1.2\times1.2\text{cm}^2$ . Note that width and length of the two plates is not equal and about  $0.2\times1.6\text{cm}^2$  free spaces was used for spot welding between the adjacent cells. In total, ten anode flow field plates and ten cathode flow field plates were formed on the silicon wafer.

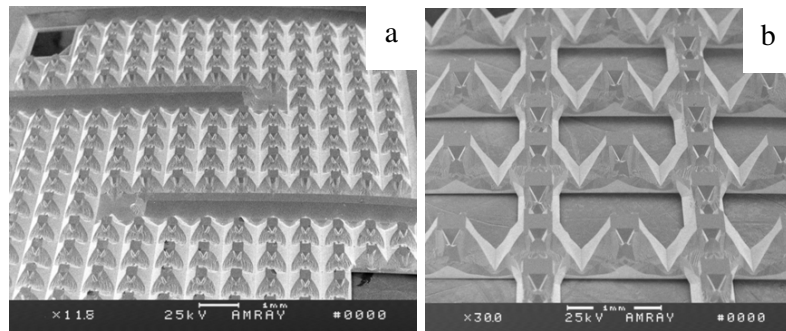


**Figure 2.** The SEM pictures of the anode and cathode flow field plates fabricated. (a) anode, (b) cathode

### 2.3. Make of the fuel buffer/distributor

A MEMS etching and bonding technology were applied to make the fuel buffer/distributor. First, using the similar wet etching method described above, a strip chamber with dimensions of about  $43\text{mm}$  long,  $11\text{mm}$  wide and  $100\mu\text{m}$  deep was formed on the front side of another piece of silicon wafer with  $350\mu\text{m}$  thickness. This chamber will act as fuel (hydrogen) buffer/distributor. A C-type channel, a fuel feed hole and a square outlet hole were fabricated at the same time. The C-type channel is about  $3\text{mm}$  wide and  $100\mu\text{m}$  deep. The C-type channel will collect exhaust gases from the 6 cells and drain them out from the outlet hole. The fuel feed hole and outlet hole are  $2.5\text{mm}$  wide. Second, a single side polished. A piece of Pyrex glass with  $500\mu\text{m}$  thickness was ultrasonically drilled to form 12 through holes with  $2\text{mm}$  in diameter. The silicon/glass bonding was applied then in the bonding machine with  $400\text{V}$  working voltage for about  $15\text{minutes}$ , and the bonding temperature was controlled at about  $800^\circ\text{C}$ . Note again that 6 of the 12 through holes were designed to act as the single cells’ feed hole and the remains outlet holes respectively. The picture of the final bonded fuel buffer/distributor is given in Fig. 3.

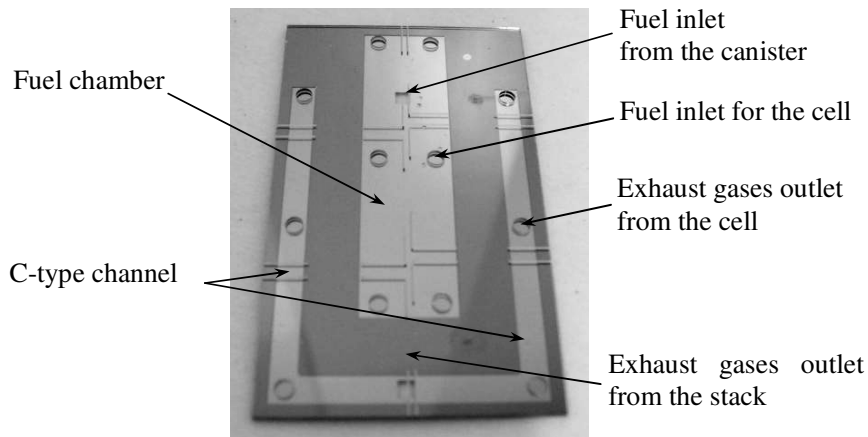


**Figure 3.** Image of the fuel buffer/distributor fabricated based on MEMS silicon-glass bonding technology

#### 2.4. Assembly of the stack

Prior to assemble the single cells, a homemade membrane-electrode-assembly (MEA, with Pt loading  $0.3\text{mg}/\text{cm}^2$  for anode and  $0.5\text{mg}/\text{cm}^2$  for cathode respectively; Nafion112 was used as separate membrane) was cut into 6 pieces with the dimension of  $1.4\text{cm}\times 1.4\text{cm}$ . In order to prevent short-circuited, the cut MEAs were ultrasonically agitated in deionized water for several seconds to remove the residential conductive materials on the cut sides.

To assemble the single cell, a MEA was sandwiched between the anode and cathode plates and pressed for about 12 hours by an electronic spiral micrometer. A kind of Epoxy resin was used to seal the cell and act as a bonding agent between the MEA and the plates.

The assembled cells were then one by one mounted on the fuel buffer/distributor with the cathode facing up. All the void space between the cells and the glasses was filled with epoxy resin seals to guarantee no gas leakage and good sealing. Work of assembling the 6-cell stack was finally completed by spot welding the adjacent cells to make them electrically conductive. The stack is about  $4.0\text{ml}$  in volume. The picture of the finally assembled stack is shown in Fig. 4.

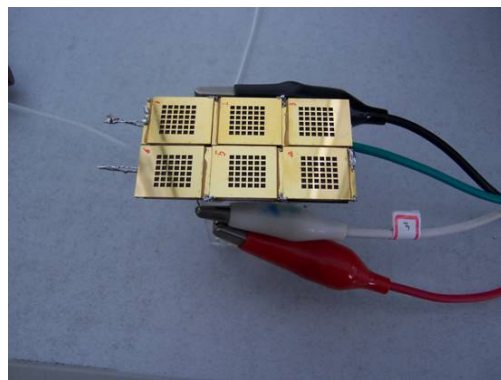


**Figure 4.** Image of the assembled stack under testing

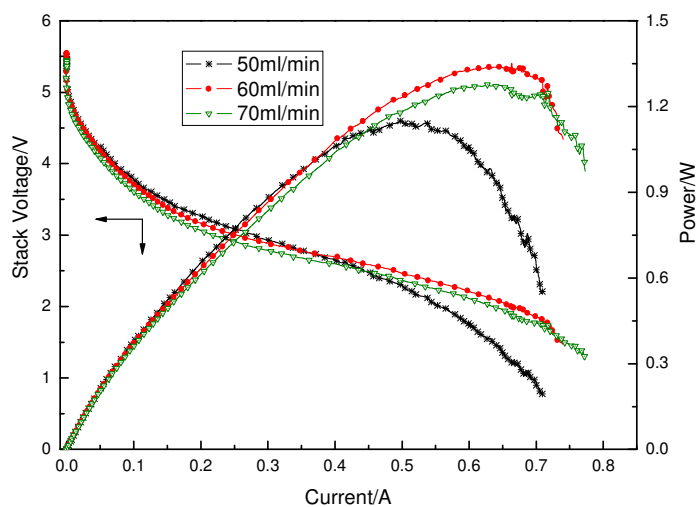
### 2.5. Performance and electrochemical resistance characterization of the stack

Performance characterization was carried out through the Arbin FCTs fuel cell instrument. Before collecting data, the stack was allowed to be activated for at least one hour at a current density of  $35\text{mA/cm}^2$ . The stack was operated on dry hydrogen at atmospheric pressure and air-breathing at  $20\pm3^\circ\text{C}$  and  $50\pm3\%$  RH.

Impedance measurements were carried out using a Solartron SI 1287 electrochemical analyzer combined with a Solartron 1255B frequency interface and Zview 3.0 software. The instrument used in potentiostatic mode with amplitude 40mV over a frequency range from 0.1 Hz to 100,000Hz, covered with 10 points per decade. Nyquist plot in our impedance measurement exhibited a typical semi-circle behavior. The left point of intersection with  $x$  axis corresponds to ohmic resistance.

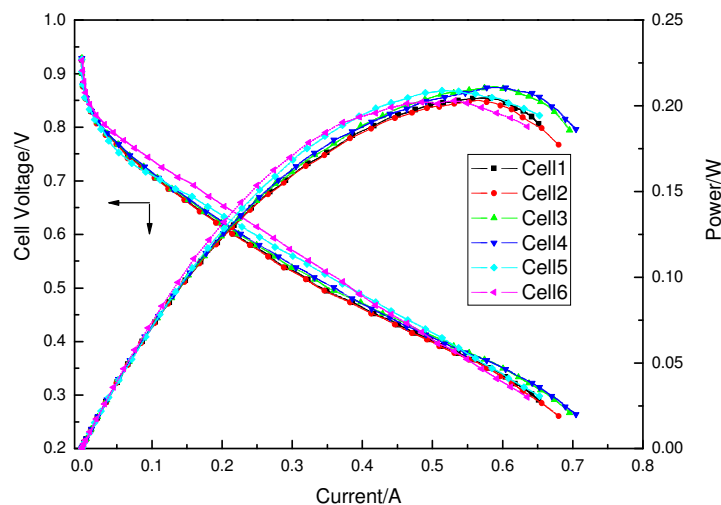
## 3. RESULTS AND DISCUSSION

Fig. 5 shows the linear polarization curve of the stack at different hydrogen flow rates of 50, 60 and 70ml/min respectively (scan rate:  $v= 0.005\text{A/s}$ ). It can be seen that the shape of stack voltage versus current curve is similar as compared with the other PEMFC stack. Usually, the curve is divided into three segments by its different voltage drop rates, which correspond to the different electrochemical processes [17]. The initial drop of the polarization curve at a very low current was due to the electrochemical activation process, which was caused by the sluggish kinetics of oxygen reduction at the cathode. The subsequent linear decrease of the polarization curve was due to an ohmic loss which is attributed to the ion flow through the electrolyte membrane, the electron flow through the electrode materials, flow field plates and current collector. The last drop was due to a diffusive loss caused by mass transfer difficulty of reactants, oxygen in most cases. However, it also can be seen



**Figure 5.** The linear polarization curve of the stack with different hydrogen flow rates under conditions:  $\text{An/Ca} = 0.3/0.5\text{mg Pt/cm}^2$ ,  $T_{cell} = 20\pm3^\circ\text{C}$  @  $50\pm3\%$  RH,  $P$  = atmospheric, and air-breathing for Cathode

from Fig. 5 that the stack's performance had some discrepancy with different hydrogen flow rates. When current is less than 0.1A, the corresponding output power had little difference; but such is not the case with further current increase, that is, at the region of 0.45~0.73A, the difference became more obvious and bigger. This could be explained by the following two negative/positive factors combined that the inner pressure of the stack and the diffusive rate of fuel for reaction went up simultaneously with the flow rate increase. So as can be expected, the moderate flow rate of 60ml/min gave the highest output power of 1.34W. The peak power density of 335W/l can be calculated out based on the volume of the stack.



**Figure 6.** The linear polarization curve of the stack with different hydrogen flow rates under conditions:  $\text{An/Ca} = 0.3/0.5\text{mg Pt/cm}^2$ ,  $T_{cell} = 20 \pm 3^\circ\text{C}$  @  $50 \pm 3\%$  RH,  $P$  = atmospheric, and air-breathing for Cathode

Fig. 6 shows the single cells' performance under the same conditions of Fig. 5. It is evident that all the 6 cells had a similar performance which is attributed to the even fuel distribution among each cells benefiting from the novel structure design of the stack. Table 1 list out internal resistances and peak power density of the 6 cells. Also, it can be seen that they were even distributed.

**Table 1.** Internal resistance and peak power density of the single cells

Factor	calculated value					
Resistance, $\Omega$	0.5087	0.5100	0.4910	0.4995	0.5028	0.5123
Peak power density, $\text{W/cm}^2$	142.4	141.7	147.2	145.8	145.1	141.0

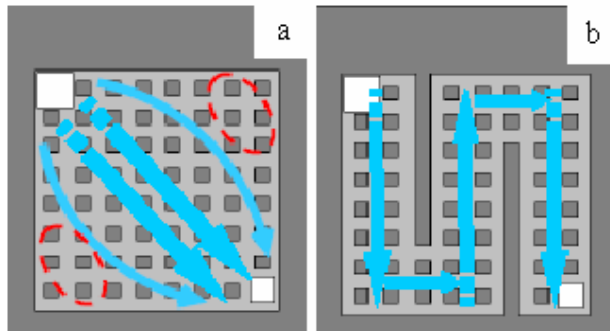


**Figure 7.** The schematic diagram of fuel flow road in Z-type and full pin-type anode flow field plates (a) full pin-typed, (b) Z-typed

Performance improvement of the stack using the novel Z-type anode flow field plates was schematically shown in Fig. 7 (b). Compared with the full pin-type flow field of anode we previously designed (see Fig. 7 (a)), the novel type flow field can make fuel flow forcedly along Z-type road. This could mean that the fuel can reach the corner of the cells to the greatest extent, while the red circle marked place in Fig. 7 (a) probably not. Under the similar conditions of operation, the stack's output peak power had about 49% enhancement when the novel Z-type anode flow field plates were used to assemble the stack. More even fuel distribution among each cell probably had the greatest contribution for the improvement. Further work is to confirm the consequence and investigate other detailed information such as heat and water management.

#### 4. CONCLUSIONS

Design, fabrication and performance characterization of a miniature 6-cell PEMFC stack with volume of 4.0ml was presented. The stack based on MEMS technology had a novel structure. A novel type of Z-type anode flow field plates were applied to replace the full pin-type ones used previously and all the single cells were assembled in the same plane with a fuel buffer/distributor as their support. Operating on dry H<sub>2</sub> and air-breathing conditions at 20±3°C and 50±3% RH, the stack produced the peak power of 1.34W and the estimated maximum power density of the stack could reach 335W/L when the stack's volume of 4.0ml was considered. Meanwhile, all the single cells in the stack performed well and even based on *V-I* and internal resistance measurement (EIS). The results suggested that the stack's performance was greatly improved. The novel flow field leading to more even fuel distribution among each cell probably had the greatest contribution for the improvement.

#### ACKNOWLEDGEMENTS

The authors gratefully acknowledge financial support from the National '863' High Technology program (No.2006AA04Z342), China.

#### References

1. Y. Yamazaki, *Electrochimica Acta* 50 (2004) 663.

2. G..Q. Lu, C.Y. Wang, T.J. Yen, X. Zhang, *Electrochimica Acta* 49 (2004) 821.
3. S.C. Yao, X.D. Tang, C.C. Hsieh, Y. Alyousef, M. Vladimer, G.K. Fedder, H.Cristina, *Energy* 31 (2006) 636.
4. J. Yeom, R.S. Jayashree, C. Rastogi, M.A. Shannon, P.J.A. Kenis. *J Power Sources* 160 (2006)1058.
5. M. Shinji, M. Mohamed, M. Toshiyuki, S. Shuichi, O. Tetsuya. *Electrochemistry Communications* 6 (2004) 562.
6. H.L. Maynard, J.P. Meyers, *J. Vac. Sci. Technol. B* 20 (2002) 1287.
7. S. Tanaka, K.S. Chang, K.B. Min, D. Satoh, K. Yoshida, M. Esashi, *Chemical Engineering J* 101(2004) 143.
8. S.C. Kelley, G..A. Deluga, W.H. Smyrl. *AICHE J.* 48 (2002) 1071.
9. J.R. Yu, P. Cheng, Z.Q. Ma, B.L. Yi, *J Power Sources* 124 (2003) 40.
10. S.C. Kelley, G..A. Deluga, W.H. Smyrl. *Electrochem. Solid State* 3 (2000)407.
11. A. Heinzel, C. Hebling, M. Müller, M. Zedda, C. Müller, *J Power Sources* 105 (2002) 250.
12. T. Kim, S. Kwon, *Chemical Engineering J* 123 (2006) 93.
13. J.D. Holladay, E.O. Jones, M. Phelps, J.L. Hu, *J Power Sources* 108 (2002) 21.
14. S.J. Lee, A. Chang-Chien, S.W. Cha, R. O' Hayre, Y.I. Park, Y. Saito, F.B. Prinz, *J Power Sources* 112 (2002)410.
15. J.R. Yu, P. Cheng, Z.Q. Ma, B.L. Yi, *Electrochimica Acta* 48 (2003) 1537.
16. R. Hahn, S. Wagner, A. Schmitz, H. Reichl, *J Power Sources* 131 (2004)73.
17. J. Larminie and A. Dicks, Fuel Cell System Explained, 2nd ed. New York, Wiley, 2002.